Medial positioning of the hippocampus and hippocampal fissure volume in Developmental Topographical Disorientation

Agustina Fragueiro, Claire Cury, Federica Santacroce, Ford Burles, Giuseppe Iaria, Giorgia Committeri

Medial positioning of the hippocampus and hippocampal fissure volume in Developmental Topographical Disorientation

Agustina, Fragueiro[1]; Claire, Cury[1]; Federica, Santacroce[2]; Ford, Burles[3]; Giuseppe, Iaria[3]; Giorgia, Committeri[2]

[1]Univ Rennes, CNRS, Inria, Inserm, IRISA UMR 6074, Empenn - ERL U 1228, F-35000 Rennes, France.
[2]Department of Neuroscience, Imaging and Clinical Sciences, University G. d'Annunzio of Chieti-Pescara, Italy.
[3]Department of Psychology, University of Calgary, Calgary, AB, Canada.

Corresponding author
Agustina Fragueiro
Empenn team, IRISA/Inria Rennes Bretagne Atlantique
Campus de Beaulieu, 35042, Rennes Cedex, France
Phone: +33 2 99 84 71 00
E-mail: agustina.fragueiro@inria.fr

Conflict of interest statement
The authors have no conflict of interest to declare.

Data availability statement
Data corresponding to the first control group are available in open access by the Human Connectome Dataset WU-Minn (Van Essen et al., 2013). Data from the developmental topographical disorientation and the second control group are not publicly available due to privacy and ethical restrictions.

Abstract

Developmental Topographical Disorientation (DTD) refers to the lifelong inability to orient by means of cognitive maps in familiar surroundings despite otherwise well-preserved general cognitive functions, and the absence of any acquired brain injury or neurological condition. While reduced functional connectivity between the hippocampus and other brain regions has been reported in DTD individuals, no structural differences in grey matter tissue for the whole brain neither for the hippocampus were detected. Considering that the human hippocampus is the main structure associated with cognitive map-based navigation, here, we investigated differences in morphological and morphometric hippocampal features between individuals affected by DTD (N=20) and healthy controls (N=238). Specifically, we focused on a developmental anomaly of the hippocampus that is characterized by the incomplete infolding of hippocampal subfields during foetal development, giving the hippocampus a more round or pyramidal shape, called Incomplete Hippocampal Inversion (IHI). We rated IHI according to standard criteria and extracted hippocampal subfield volumes after FreeSurfer's automatic segmentation.

We observed similar IHI prevalence in the group of individuals with DTD with respect to the control population. Neither differences in whole hippocampal nor major hippocampal subfield volumes have been observed between groups. However, when assessing the IHI independent criteria, we observed that the hippocampus in the DTD group is more medially positioned comparing to the control group. In addition, we observed bigger hippocampal fissure volume for the DTD comparing to the control group. Both of these findings were stronger for the right hippocampus comparing to the left.

Our results provide new insights regarding the hippocampal morphology of individuals affected by DTD, highlighting the role of structural anomalies during early prenatal development in line with the developmental nature of the spatial disorientation deficit.

Keywords: hippocampus, incomplete hippocampal inversion, developmental topographical disorientation, spatial navigation, hippocampal fissure, subiculum, subfields automatic segmentation

1 Introduction

Developmental Topographical Disorientation (DTD) refers to the lifelong inability to orient in familiar surroundings despite otherwise well-preserved general cognitive functions, and the absence of any acquired brain injury or neurological condition (Iaria & Burles, 2016). Individuals with DTD are unable to orient by means of cognitive maps in both ecological (Bianchini et al., 2010; Iaria et al., 2009) and virtual (Bianchini et al., 2014; Iaria & Barton, 2010) environments. This inability to orient by means of cognitive maps suggests that the neural mechanisms related to the presence of DTD may involve the hippocampus, a region in the medial temporal lobe that is critical for the formation and use of cognitive maps in both human and non-human animals (Bottini & Doeller, 2020; Hartley et al., 2003; Iaria et al., 2007; O'Keefe & Nadel, 1978).

Few studies have investigated the functional and structural properties of the hippocampus in individuals affected by DTD. Iaria and colleagues (2014) reported reduced functional connectivity between the right hippocampus and the prefrontal cortex in this population. In addition, a DTD case study using functional and diffusion tensor imaging (Kim et al., 2015) has reported an atypical response profile in the retrosplenial cortex that presented with a decreased functional coupling with the parahippocampal place area, which was, however, not related to compromised structural connectivity. Furthermore, no structural differences in grey matter tissue for the whole brain neither for the hippocampus were detected when using voxel-based morphometry (Iaria et al., 2014). Thus, while reduced functional connectivity has been observed in DTD, no structural differences have been reported till now.

On the other hand, there is evidence of a developmental anomaly of the hippocampus that is characterized by the incomplete infolding of hippocampal subfields before gestational week 21 (Bajic et al., 2008; Fu et al., 2021). This structural anomaly during development gives the hippocampus a more round or pyramidal shape, and is referred to as hippocampal malrotation or incomplete hippocampal inversion (IHI). As the development stopped, IHI hippocampi resemble the foetal shape and remain more medially located with a deeper collateral sulcus. Along normal development, before week 16, the subiculum region is larger and more medially positioned, and subfields CA1, CA2 and CA3 are arranged linearly before adopting the characteristic arc shape. Only by weeks 18–21, the dentate gyrus and CA embed into the temporal lobe, with CA1–3 subfields forming an arc (Kier et al., 1997). The incompletion of this process results in the IHI characteristic shape, which occurs predominantly in the left hippocampus (Cury et al., 2015). Although it is considered one extreme of the normal phenotypic spectrum, it is more prevalent in epilepsy and it is thought to be a factor of susceptibility for hippocampal sclerosis (Bernasconi et al., 2005). It has been associated with larger subiculum volumes and smaller CA1 volumes in healthy young adults (Fragueiro et al., 2023), to smaller CA1 and right CA3 volumes in healthy aging (Colenutt et al., 2018), and to extra-hippocampal morphological changes in sulci mainly located in occipito-temporal cortices (Cury et al., 2015). A genome-wide association study on adolescence evidenced correlations between IHI and genetic traits associated either with intelligence or education attainment (Cury et al., 2020), however, it remains unclear whether IHI is related to cognitive impairments, in particular to those related to hippocampal function (Stiers et al., 2010). Interestingly, it has been proposed that IHI could be a genetic developmental imaging feature that may represent a more diffuse but subtle structural atypicality during brain development (Fu et al., 2021).

Here, we investigated differences in morphological and morphometric hippocampal features between individuals affected by DTD and healthy controls. Considering that the hippocampus is the main structure involved in the generation and use of cognitive maps, as well as, that DTD and IHI are both developmental features, we proposed to explore if there may be an association among their presence. To this aim, we rated IHI according to Cury et al. (2015) criteria and we extracted hippocampal subfield volumes after their automatic segmentation to compare DTD to control individuals.

2 Materials and methods

2.1 Participants

2.1.1 *DTD group.* The DTD group included 20 females right-handed individuals (age range 25 to 64 years) recruited locally through a public advertising campaign. These individuals reported no psychiatric or neurological disorders, they all had normal or corrected-to-normal vision, and were all diagnosed with DTD following the criteria described in previous studies (Burles & Iaria, 2020). These criteria are: (1) having experienced the inability of orient, and therefore getting lost, from childhood, (2) experiencing getting lost in extremely familiar surroundings, (3) despite having no other cognitive complaints, and (4) in the absence of any other cognitive or neurological condition. All participants provided written informed consent as approved by the local research ethics board of the University of Calgary (REB14-2176). These individuals were included in the study following a visual examination for quality issues.

2.1.2 *Healthy Control group 1 (HC1).* The first HC group consisted of 220 healthy females, 213 of them with an age range = 26 to 30 years and 7 of them with an age over 36. All of them are part of the Human Connectome Dataset WU-Minn (Van Essen et al., 2013). These individuals were included in the study following exclusion of participants with quality control issues (as reported on the database), major neurological diseases, and psychiatric or medical disorders.

2.1.3 *Healthy Control group 2 (HC2).* To exclude scanner-related differences between groups, we included 18 females (age range 25 to 64) whose images were acquired with the same protocol that the DTD group. These individuals reported no psychiatric or neurological disorders, they all had normal or corrected-to-normal vision, and were assessed as no-DTD according to the criteria described in previous studies (Burles & Iaria, 2020). All participants provided written informed consent as approved by the local research ethics board of the University of Calgary (REB14-2176). These individuals were included in the study following a visual examination for quality issues.

A summary with the descriptive information of all groups can be found in Table 1.

2.2 MRI data

2.2.1 *DTD and HC2 databases.* Participants were scanned using a 3T GE Discovery 750 MRI with an eight-channel head coil. Twenty-two individuals (DTD=9, HC2=13) were scanned in 2011 and 2013, and anatomical images were acquired using a T1-weighted SPGR sequence (Minimum Full TE, 11° flip angle, 1 mm isotropic voxels, 25.6 cm FOV). Sixteen additional individuals (DTD=11, HC2=5) were scanned in the same scanner in 2017, with anatomical images acquired using a T1-weighted fast SPGR sequence (Minimum Full TE, 10° flip angle, 1 mm isotropic voxels, 25.6 cm FOV, ARC factor 2).

2.2.2 *HC1 database.* All HC participants were scanned on a customized Siemens 3T "Connectome Skyra" housed at Washington University in St. Louis, using a standard 32-channel Siemens head coil and a body transmission coil designed by Siemens using the gradients of the WU-Minn and MGH-UCLA Connectome scanners. T1-weighted 3D MPRAGE were acquired with TR=2400 ms, TE=2.14 ms, TI=1000 ms, 8° flip angle, FOV=224x224, 0.7 mm isotropic voxel, bandwidth=210 Hz/px, iPAT=2, and acquisition time=7:40 (min:sec).

2.3 Incomplete Hippocampal Inversion rating

T1-weighted images were linearly transformed to MNI using *flirt* in FSL 6.0.5.1 in order to perform the assessment with a standardized orientation between subjects. The software medInria (https://med.inria.fr/) (Vichot et al., 2012) was used to rate IHI, according to the criteria reported in Cury et al. (2015), in 220

brains from the HC1, 18 brains from the HC2 and 20 from the DTD group. Note that all individual criteria C1, C2, C3, and C5 were rated independently. C1 assesses the roundness and verticality of the hippocampal body, with a score of 0 for flat and horizontal hippocampi and, on the other extreme, a maximum score of 2 for an oval and vertical hippocampus. C2 assesses the verticality and depth of the collateral sulcus relatively to the size of the hippocampus, with a score of 0 for a horizontal collateral sulcus not crossing the lateral limit of the hippocampus, and a maximum score of 2 if the sulcus surpasses the limit of the hippocampus and has a vertical orientation. C3 judges the medial positioning of the hippocampus, assessed by the length of the part of the subiculum that is not covered by the dentate gyrus relatively to the lateral part of the CA/subiculum that is covered by the dentate gyrus. Even in particular cases of variability in subfields location or orientation, the two segments were always defined orthogonally to the brain midline at the level of the superior bend of the subiculum. In addition, C3 considers whether there is visible presence of cerebrospinal fluid in the temporal horn of the lateral ventricle laterally to the hippocampus, or not, with higher scores for the first case (i.e. visible cerebrospinal fluid). C5 evaluates the depth of both the collateral and the occipitotemporal sulcus with respect of the subiculum, with a score of 0 if none of the sulci exceeds the level of the subiculum and a maximum score of 2 if at least one of the sulci exceeds vertically the superior limit of the subiculum. A total IHI score (going from 0 to 8) was calculated for each hemisphere by summing all criteria. If the total score exceeded 3.75, the hemisphere was classified as IHI. Criteria 4 was not rated as recommended in Cury et al 2015, since this criterion is not well defined in the literature and therefore not comparable across studies.

Before starting the rating, we evaluated intra- and inter-rater agreement. For intra-rater coherence, AF rated the same database of 30 subjects randomly extracted from the Human Connectome Project database (age 26-30) with a distance of 15 days. For inter-rater agreement, CC rated the same 30 subjects. AF and FS blindly rated 40 participants (20 from the DTD database and 20 randomly selected from the HC1 database). Finally, AF rated the 18 participants from the HC2. Kappa scores were calculated for C5, and kappa weight scores were calculated for criteria C1, C2, and C3. All intra- and inter-rater scores were assessed independently for each hemisphere and all of them were above 0.65 (Table 2).

2.4 Hippocampal subfields segmentation

The tool for segmentation of hippocampal subfields offered by FreeSurfer 7 was run using the T1-weighted scans after applying *recon-all* method. All process steps were applied, including motion correction, intensity normalization, Talairach transformation, among others (for the complete details see https://surfer.nmr.mgh.harvard.edu/fswiki/recon-all). The tool (*segmentHA_T1*) segments the different subfields by using a Bayesian inference approach based on image intensities and prior knowledge of a probabilistic atlas which was generated from in vivo manual segmentations and ultra-high-resolution ex vivo MRI data of the hippocampal substructures (Iglesias et al., 2016).

The segmented subfields with this method followed the head-body-tail subdivision (Iglesias et al., 2015) and are: CA1 body, CA1 head, CA2/3 head, CA2/3 body, CA4 head, CA4 body, fimbria, granule cell layer of dentate gyrus (GC-ML-DG) head, GC-ML-DG body, hippocampus-amygdala-transition-area (HATA), tail, hippocampal fissure, molecular layer head, molecular layer body, parasubiculum, presubiculum head, presubiculum body, subiculum head, subiculum body (Figure 1). Volumes in mm^3 for each subfield were obtained through FreeSurfer (*quantifyHAsubregions*) and corrected by whole brain volume calculated on FSL (*fslstats*).

2.5 Pre-analyses for sanity check

2.5.1 *Age-effect control:* Data were analysed with the Kolmogorov-Smirnov Test. As not all variables were normally distributed, we conducted non-parametric statistics. As the HC1 database provided age-range but

not each individual subject age, the following analyses on age were conducted on participants from the HC2 (N=18) and the DTD (N=20) groups. To test for an age effect on IHI, we conducted Spearman's correlations between age and IHI global scores for each hemisphere independently. To test for an age effect on volumes, we conducted Spearman's correlations between age and volumes for the following subfields of interest: CA1, CA2+3+4+DG, complete subiculum (including presubiculum, parasubiculum and subiculum), hippocampal fissure, and tail. Head and body sections were added together for each subfield of interest. Correlations between age and whole hippocampal head, whole hippocampal body and whole hippocampal volume were also tested.

2.5.2 *Scanner-effect on IHI:* To test for scanner related differences that may affect IHI rating, we first compared HC1 (N=220) and HC2 (N=18) groups. Mann-Whitney tests for independent samples between groups were conducted for all criteria independently and for the global IHI score. Each hemisphere was tested independently. P-values were corrected for multiple comparisons using Bonferroni correction (x10 tests).

2.5.3 *Scanner-effect on volumes:* To test for scanner-related differences that may impact the automatic segmentation of hippocampal subfields (for examples of segmentations for all three groups see Supplementary Figure 1), we conducted Mann-Whitney tests between HC1 (N=219, as segmentation failed for 1 subject) and HC2 (N=18) for the subfields of interest (CA1, CA2+3+4+DG, complete subiculum, hippocampal fissure, and tail), for whole hippocampal head, whole hippocampal body and whole hippocampus volume. Each hemisphere was tested independently. P-values were corrected for multiple comparisons using Bonferroni correction (x16 tests).

Considering that IHI may impact hippocampal automatic segmentation (Kim et al., 2012), we finally repeated the same analyses but excluding IHI hippocampi for each hemisphere independently. We conducted Mann-Whitney tests between HC1 (N=177) and HC2 (N=14) for the left hemisphere after excluding left IHI participants. The same analyses were conducted for the right hemisphere after excluding right IHI hippocampi (HC1=205, HC2=16). P-values were corrected for multiple comparisons using Bonferroni correction (x16 tests).

2.6 Pre-analyses results

2.6.1 Age-effect. No significant correlation was observed between age and IHI scores for any hemisphere (Figure 2A), neither between age and any subfield or whole hippocampal volumes (Figure 2B). The complete list of correlation's coefficients and uncorrected p-values is reported in Table 3.

2.6.2 Scanner-effect on IHI. In the HC1 database (N=213, age range = 26 to 30 years; N=7, age>36), we rated as IHI 19% (N=42) of hippocampi in the left hemisphere and 6% (N=14) of hippocampi in the right hemisphere; a 4% of brains were identified as IHI bilaterally. In the HC2 group (N=18, age 25 to 64), we rated as IHI 22% (N=4) of hippocampi in the left hemisphere and 11% (N=2) of hippocampi in the right hemisphere; a 5% of brains were identified as IHI bilaterally. The rates of IHI prevalence in both HC1 and HC2 groups are similar to those previously reported in the healthy population in other studies (Cury et al., 2015; Colenutt et al., 2018). No significant difference was evidenced between HC1 and HC2 for any independent criterion (C1, C2, C3, C5) neither for the global IHI score (Left IHI score: U=1830, corrected p>1; Right IHI score: U=1784.5, corrected p>1) (Figure 3A). For the subsequent analyses on IHI, we merged HC1 and HC2 in one healthy control group (HC, N=238).

2.6.3 Scanner-effect on volumes. We observed a difference between HC1 and HC2 groups for the right subiculum (U=1108, corrected p=0.032) and a strong tendency for the left fissure (U=1145, corrected p=0.0501) (Figure 5A). When repeating the same analyses but excluding IHI hippocampi for each hemisphere independently, no significant difference was observed (Right subiculum: U=1014, corrected p=0.353; Left fissure: U=706, corrected p=0.237). For the subsequent analyses on volumes, we merged HC1

and HC2 in one healthy control group, first without excluding IHI (HC, N=237), but after we repeated the analysis excluding IHI for each hemisphere independently (left: DTD=15, HC=191; right: DTD=18, HC=221).

2.6.4 Conclusion on the pre-analyses for sanity check. After conducting these pre-analyses for a sanity check of our data, we safely merged HC1 and HC2 in one HC group including a broader age-range and images acquired with the two different scanners. Furthermore, due to the tendency for a scanner-effect observed for the subiculum and fissure, if any difference between HC and DTD groups would be found for these subfields, analyses would be replicated including only HC2 as control group, as it shares the same scanner than the DTD group.

2.7 Statistical Analyses

2.7.1 *IHI scores.* We conducted Mann-Whitney tests for independent samples between HC (N=238) and DTD (N=20) groups for all criteria independently and for the global IHI score. Hemispheres were tested independently. P-values were corrected for multiple comparisons using Bonferroni correction (x10 tests).

2.7.2 *Volumes.* We conducted Mann-Whitney tests comparing the whole HC (N=237) group with the DTD (N=20) group for the subfields of interest (CA1, CA2+3+4+DG, subiculum, hippocampal fissure, and tail), whole hippocampal head, whole hippocampal body and whole hippocampal volume. Each hemisphere was tested independently. P-values were corrected for multiple comparisons using Bonferroni correction (x16 tests).

In addition, we repeated the same analyses but excluding IHI hippocampi for each hemisphere independently. We conducted Mann-Whitney tests between HC (N=191) and DTD (N=15) for the left hemisphere after excluding left IHI participants. The same analyses were conducted for the right hemisphere after excluding right IHI hippocampi (HC=221, DTD=18). P-values were corrected for multiple comparisons using Bonferroni correction (x16 tests).

Finally, considering the tendency observed for a scanner effect in the left hippocampal fissure segmentation, we conducted Mann-Whitney tests to compare fissure volumes between both groups acquired with the same scanner, thus, between DTD (N=20) and HC2 (N=18). Each hemisphere was tested independently. P-values were Bonferroni corrected (x2 tests).

All statistical analyses on this study, for both IHI and volumes, were conducted on IBM SPSS Statistics 25. Violin plots (figures 3, 5 and 6), boxplots (figures 5 and 6) and dot plots (figure 6) were performed using *ggplot2* (Wickham, 2009) in RStudio running on R version 4.2.1 (2022-06-23 ucrt).

3 Results

3.1 IHI occurrence in HC and DTD group

For the DTD database (N=20), we rated as IHI 25% (N=5) of hippocampi in the left hemisphere and 10% (N=2) of hippocampi in the right hemisphere; a 10% of brains were identified as bilateral IHI. The rates of IHI prevalence in the DTD group are similar to both control groups (HC1 and HC2) and to those previously reported in the healthy population in other studies (Cury et al., 2015; Colenutt et al., 2018).

When observing each criteria independently, a significant difference was evidenced between HC and DTD groups for C3 in both the right (U=1297.5, corrected p=0.003) and left hippocampus (U=1472, corrected p=0.027) (Figure 3B), meaning that the hippocampus is more medially positioned for DTD participants as compared to HC (Figure 4), with a more significant effect for the right hemisphere comparing to the left. No significant differences were evidenced for criteria 1, 2 or 5, neither for the total IHI score.

3.2 Volumetric measures in HC and DTD groups

When comparing volumes between the HC and the DTD groups, significant differences were observed only for the hippocampal fissure bilaterally (Left: U=771, corrected p=0.000009; Right: U=793, corrected p=0.00001), with higher fissure volumes for the DTD group (Figure 5B). No significant differences were evidenced for the other subfields of interest, neither for whole head, body or whole hippocampal volumes.

Due to the scanner effect previously observed for some specific subfields (right subiculum and left fissure), and taking into consideration that IHI may affect hippocampal automatic segmentation (Kim et al., 2012), we repeated the analyses comparing HC and DTD groups but now excluding IHI hippocampi independently for each hemisphere. The difference for hippocampal fissure volume remained significant for both hemispheres (Left: U=467, corrected p=0.0002; Right: U=699, corrected p=0.00008).

Finally, when comparing fissure volumes between the two groups acquired with the same scanners (DTD vs HC2), we observed that the difference remained significant for the right hippocampal fissure (U=86, corrected p=0.01) but not for the left (U=125, corrected p=0.224) (Figure 6).

4 Discussion

We observed similar IHI prevalence in a group of individuals with DTD with respect to a control population. Neither differences in whole hippocampal or major hippocampal subfield (head, body, CA, subiculum, tail) volumes have been evidenced between groups. Thus, in agreement with previous studies, no major morphological nor volumetric differences are reported for DTD subjects. However, when assessing IHI criteria independently, we observed that the hippocampus in the DTD group is more medially positioned comparing to the control group, meaning a shorter distance of the medial part of the subiculum not covered by the dentate gyrus relatively to the more lateral part of CA/subiculum that is covered by the dentate gyrus (Cury et al., 2015). Volumetric analyses allowed us to determine that this medial positioning is not associated to a smaller subiculum structure, which has the same volume between groups. Interestingly, this specific medial portion of the hippocampal formation (i.e. the subiculum), located between the hippocampus proper and the parahippocampal region, has been defined as the "heart of the extended hippocampal system" (Aggleton & Christiansen, 2015), as it is the main origin for the largest array of extrinsic hippocampal efferents, be they cortical or subcortical, in rodents (Witter et al., 2006) and primates (Aggleton, 2012). Thus, the subiculum is the principal source of many of the hippocampal projections to cortical targets that are critically implicated in multiple forms of spatial cognition and memory (Morris et al., 1990; Naber et al., 2000; Sun et al., 2019). As well, it influences the hippocampus directly via inputs to the CA1, and indirectly via projections to the entorhinal cortex (Commins et al., 2002; Swanson & Cowan, 1977).

The subiculum connections display a complex topography that has be divided in "proximal" and "distal" subiculum, distinguishing locations within the transverse plane of the subiculum with different functions (Aggleton & Christiansen, 2015; Witter et al., 2006). This subdivision of the subiculum, assumes that the dentate gyrus lies at the core of the structure, and if the structure is unrolled, "proximal" refers to tissue closer to the centre of the hippocampus reaching the border of CA1, while "distal" refers to the further tissue that limits with the presubiculum. The proximal subiculum is preferentially linked with the perirhinal cortex, lateral entorhinal cortex in rats or rostral and medial entorhinal cortex in primates, prefrontal cortex, amygdala, and nucleus accumbens, and it is more involved in processing object-based information. Meanwhile, the distal subiculum (located more medially, right before the presubiculum) is reciprocally interconnected with the medial entorhinal cortex in rats, the caudal and lateral entorhinal cortex in primates,

and parahippocampal cortices. This distal portion of the subiculum has been involved in processing spatial information, reflecting their parahippocampal cortex connections (Aggleton, 2012; Witter et al., 2000).

In the same line, the CA1/proximal subiculum and the distal subiculum/presubiculum areas have been proposed to be 'hotspots' of anatomical connectivity for multiple cortical areas in both non-human (Kravitz et al., 2011) and human (Dalton et al., 2022) primates. A parieto–medial temporal pathway supporting spatial navigation has been indeed described as emerging from the caudal portion of the inferior parietal lobule and terminating in the parahippocampal cortex and hippocampus, through both direct and indirect projections (Kravitz et al., 2011). The direct projections arrive first to the CA1/prosubiculum, second to the pre/parasubiculum, and third, to the posterior parahippocampal areas. The indirect projections, instead, connect the same source to the same targets, relaying through the posterior cingulate and retrosplenial cortices (Kravitz et al., 2011). A recent study on structural connectivity in humans provided further evidence of the existence of discrete hubs of dense anatomical connectivity along the anterior–posterior axis of the hippocampus, one corresponding to the CA1/proximal subiculum, and another more medial corresponding to the distal subiculum/presubiculum (Dalton et al., 2022).

Accumulating evidence from neuroimaging studies has specifically involved the medial hippocampal hub (i.e. distal subiculum/pre/parasubiculum), which is targeted by visuospatial processing areas from the medial parietal and occipital cortices, in scene-based cognitive processing (Dalton & Maguire, 2017). Functional MRI studies have evidenced that the subiculum, plays a unique role in visuospatial cognition, with the anteromedial subiculum involved in the discrimination of complex scenes from different viewpoints (Hodgetts et al., 2017), and the distal portion of the subiculum implicated in scene processing and scene construction (Dalton et al., 2018), mainly due to its functional connections with the parahippocampal cortex (Grande et al., 2022). Interestingly, individuals with DTD suffer only from spatial orientation and spatial memory problems, but they do not suffer from general memory problems (Iaria & Barton, 2010), and the more medial part of the subiculum (or the distal subiculum/presubiculum), which has been rated as shorter in length (or more compress) in the DTD group comparing to the control group, has been specifically linked to visuospatial information processing. Therefore, our finding aligns with the description of different hubs of anatomical connectivity along the hippocampus associated with different cortical inputs/outputs, in agreement with studies that have emphasized the importance of considering the hippocampus as a heterogeneous structure (Aggleton & Christiansen, 2015; Dalton et al., 2022; Kravitz et al., 2011).

The cortico-hippocampal-parahippocampal communication has been proposed to be crucial for the construction and use of cognitive maps (Epstein et al., 2017). By accessing to allocentric and egocentric streams of spatial information, the parahippocampal cortex enables the construction of global representations of spatial environments (Weniger et al., 2010). Increased activity exclusively within the parahippocampal cortex, and more pronounced in the right parahippocampus, was reported during learning in a virtual maze (Weniger et al., 2010). Furthermore, a lesion study found deficits in virtual maze learning only after right parahippocampal gyrus removal covering the perirhinal, entorhinal and posterior parahippocampal cortices (Weniger & Irle, 2006). These studies stand a main role for the right parahippocampal region in spatial navigation and spatial memory, comparing to the left. Our result of a more medial positioning for the hippocampus in the DTD group, with stronger results for the right hippocampus comparing to the left, encourages volumetric and shape analyses on related medial temporal lobe structures, specifically on the subiculum and parahippocampal regions, in individuals reporting DTD. Thus, further research may investigate if the medial position of the hippocampus may be linked to atypical subiculum shape or atypical shape/volumes of parahippocampal structures. In addition, it would be of interest for further research to study if this specific morphological feature may be associated with the

reduced functional connectivity between the right hippocampus and the prefrontal cortex already reported in DTD individuals (Iaria et al., 2014).

In a second group of analyses, we observed higher hippocampal fissure volumes for the DTD comparing to the control group, mainly for the right hemisphere. The hippocampal fissure is a sulcus around which the hippocampal infolding occurs. It begins as a small indentation at the 10th week of foetal development, but between the 18th and the 21st week, it is obliterated almost completely by the fusion between CA and DG (Humphrey, 1967). The FreeSurfer method that we used to segment hippocampal subfields allowed us to obtain hippocampal fissure volumes, including the residual hippocampal cavities, which are cysts resulting from lack of hippocampal fissure obliteration that are most commonly localized laterally, at the apex of the hippocampal fold, between the CA and the DG. Hippocampal cavities mainly reflect cerebrospinal fluid collection (Yoneoka et al., 2002) and, although their presence is common on MRI scans, their clinical significance is unclear. An increased prevalence of hippocampal cavities has been reported in patients with memory disorders, and their prevalence was reported to increase with age in healthy subjects (Maller et al., 2011). On the contrary, other studies have reported a lack of association between the presence of hippocampal cavities and age, sex, or general cognitive functioning (i.e. declarative memory, executive functioning, working memory, verbal fluency, attention) (Blom et al., 2019; Uttner et al., 2011). One study has reported an enlargement of the hippocampal sulcus associated with medial temporal lobe atrophy in Alzheimer disease, but not enlargement of the hippocampal cavities (Bastos-Leite et al., 2006).

Interestingly, the criteria 3 used in our study for IHI rating, considers not only the medial positioning of the hippocampus, but also if there is presence of cerebrospinal fluid in the temporal horn of the lateral ventricle or not, with higher scores for the first case (Cury et al., 2015). Thus, the DTD group presented a more medial positioning of the hippocampus but also the presence of cerebrospinal fluid in the temporal horn laterally to the hippocampus. Therefore, increased cerebrospinal fluid was observed in the DTD group on larger hippocampal sulcus and cavities corresponding to the hippocampal fissure, but also inside the temporal horn laterally to the hippocampus.

A limitation of our study is the use of different scanners in which the images for the DTD and the big majority of the control group were acquired, which may have an impact on the automatic segmentation output. To address this issue and reduce the possibility of observing a confounding effect, we first applied the same recon-all processing to all images, and secondly, we repeated our analyses reducing factors that may introduce a segmentation bias by excluding IHI hippocampi. Finally, we included in our study a control group in which the images were acquired with the same scanner used in the DTD group. Although we have applied all these measures to control image processing quality, we acknowledge that the automatic segmentation of the hippocampal fissure remains particularly vulnerable to signal loss and distortion due to its small size, especially in lower contrast images, leading to lower reliability (Brown et al., 2020). As such, the findings reported in our study regarding the difference in hippocampal fissure volume between the DTD and the control group should be taken cautiously and encourage further research on this specific subfield through a manual segmentation approach and possibly with ultra-high definition images.

A second aspect that we would like to discuss, regards the definition of the most medial edge of the subiculum for the assessment of criteria 3. In the rating used in our study, we sat the medial edge of the medial segment at the level of the superior bend of the subiculum, and not necessarily where the cortical tissue of the temporal lobe reaches the absolute most medial extreme, which in some specific morphological variations may correspond to a lower portion of the presubiculum. Given the degree of individual variability in morphology of the medial edge of the hippocampus, we considered important to specify the criteria applied in our rating, thus, setting the two segments always orthogonally to the brain midline at the level of the superior bend of the subiculum, even in particular cases of individual variability in subfield location/orientation.

Finally, we understand that the small number of participants in the DTD group may be considered as a limitation. To address the small size of both the DTD and the HC2 groups, we opted to increase the power in our Mann Whitney analyses by including a bigger control group (merging HC1 and HC2) as representative of the general population. The broad age-range of the DTD group was taken into consideration by including also a broad age-range in the control group, after having excluded the possibility of an age-effect with the pre-analysis specifically conducted on our data.

Overall, the findings described in this study provide with the very first evidence of morphological markers in the brain of individuals affected by DTD. This is of significant impact given that, to date, there is no evidence in the literature of any neurological structural property of the brain that may confirm the presence of DTD as described by individuals experiencing this lifelong condition. A neurological marker that would confirm the presence of DTD not only helps individuals in the identification of the condition but will improve significantly the enrolment of DTDs across studies investing any aspect of this condition. As such, we are expecting that our findings will serve as stepping stones for future studies investigating the mechanisms of DTDs and their potential treatments.

In conclusion, our results provide new insights regarding the hippocampal morphology of individuals affected by DTD, whose hippocampus appear more medially positioned and present enlarged hippocampal fissure volume, thus increased intra-hippocampal cerebrospinal fluid, comparing to a control population. In line with the developmental (i.e. not acquired) nature of the spatial disorientation deficit, the present data underly the role of hippocampal structural anomalies during early prenatal development.

5 References

Aggleton, J. P. (2012). Multiple anatomical systems embedded within the primate medial temporal lobe: Implications for hippocampal function. *Neuroscience and Biobehavioral Reviews*, *36*(7), 1579–1596. https://doi.org/10.1016/j.neubiorev.2011.09.005

Aggleton, J. P., & Christiansen, K. (2015). The subiculum: The heart of the extended hippocampal system. *Progress in Brain Research*, *219*, 65–82. https://doi.org/10.1016/bs.pbr.2015.03.003

Bajic, D., Wang, C., Kumlien, E., Mattsson, P., Lundberg, S., Eeg-Olofsson, O., & Raininko, R. (2008). Incomplete inversion of the hippocampus—A common developmental anomaly. *European Radiology*, *18*(1), 138–142. https://doi.org/10.1007/s00330-007-0735-6

Bastos-Leite, A. J., van Waesberghe, J. H., Oen, A. L., van der Flier, W. M., Scheltens, P., & Barkhof, F. (2006). Hippocampal Sulcus Width and Cavities: Comparison Between Patients with Alzheimer Disease and Nondemented Elderly Subjects. *AJNR: American Journal of Neuroradiology*, *27*(10), 2141–2145.

Bernasconi, N., Kinay, D., Andermann, F., Antel, S., & Bernasconi, A. (2005). Analysis of shape and positioning of the hippocampal formation: An MRI study in patients with partial epilepsy and healthy controls. *Brain*, *128*(10), 2442–2452. https://doi.org/10.1093/brain/awh599

Bianchini, F., Incoccia, C., Palermo, L., Piccardi, L., Zompanti, L., Sabatini, U., Peran, P., & Guariglia, C. (2010). Developmental topographical disorientation in a healthy subject. *Neuropsychologia*, *48*(6), 1563–1573. https://doi.org/10.1016/j.neuropsychologia.2010.01.025

Bianchini, F., Palermo, L., Piccardi, L., Incoccia, C., Nemmi, F., Sabatini, U., & Guariglia, C. (2014). Where Am I? A new case of developmental topographical disorientation. *Journal of Neuropsychology*, *8*(1), 107–124. https://doi.org/10.1111/jnp.12007

Blom, K., Koek, H. L., van der Graaf, Y., Zwartbol, M. H. T., Wisse, L. E. M., Hendrikse, J., Biessels, G. J., Geerlings, M. I., & on behalf of the SMART Study Group. (2019). Hippocampal sulcal cavities: Prevalence, risk factors and association with cognitive performance. The SMART-Medea study and PREDICT-MR study. *Brain Imaging and Behavior*, *13*(4), 1093–1102. https://doi.org/10.1007/s11682-018-9916-y

Bottini, R., & Doeller, C. F. (2020). Knowledge Across Reference Frames: Cognitive Maps and Image Spaces. *Trends in Cognitive Sciences*, *24*(8), 606–619. https://doi.org/10.1016/j.tics.2020.05.008

Brown, E. M., Pierce, M. E., Clark, D. C., Fischl, B. R., Iglesias, J. E., Milberg, W. P., McGlinchey, R. E., & Salat, D. H. (2020). Test-retest reliability of FreeSurfer automated hippocampal subfield segmentation within and across scanners. *NeuroImage*, *210*, 116563. https://doi.org/10.1016/j.neuroimage.2020.116563

Burles, F., & Iaria, G. (2020). Behavioural and cognitive mechanisms of Developmental Topographical Disorientation. *Scientific Reports*, *10*(1), 20932. https://doi.org/10.1038/s41598-020-77759-8

Colenutt, J., McCann, B., Knight, M. J., Coulthard, E., & Kauppinen, R. A. (2018). Incomplete Hippocampal Inversion and Its Relationship to Hippocampal Subfield Volumes and Aging: Incomplete Hippocampal Inversion and Aging. *Journal of Neuroimaging*, *28*(4), 422–428. https://doi.org/10.1111/jon.12509

Commins, S., Aggleton, J. P., & O'Mara, S. M. (2002). Physiological evidence for a possible projection from dorsal subiculum to hippocampal area CA1. *Experimental Brain Research*, *146*(2), 155–160. https://doi.org/10.1007/s00221-002-1158-x

Cury, C., Scelsi, M. A., Toro, R., Frouin, V., Artiges, E., Grigis, A., Heinz, A., Lemaître, H., Martinot, J.-L., Poline, J.-B., Smolka, M. N., Walter, H., Schumann, G., Altmann, A., Colliot, O., & IMAGEN Consortium. (2020).

Genome wide association study of incomplete hippocampal inversion in adolescents. *PloS One*, *15*(1), e0227355. https://doi.org/10.1371/journal.pone.0227355

Cury, C., Toro, R., Cohen, F., Fischer, C., Mhaya, A., Samper-González, J., Hasboun, D., Mangin, J.-F., Banaschewski, T., Bokde, A. L. W., Bromberg, U., Buechel, C., Cattrell, A., Conrod, P., Flor, H., Gallinat, J., Garavan, H., Gowland, P., Heinz, A., … Colliot, O. (2015). Incomplete Hippocampal Inversion: A Comprehensive MRI Study of Over 2000 Subjects. *Frontiers in Neuroanatomy*, *9*. https://doi.org/10.3389/fnana.2015.00160

Dalton, M. A., D'Souza, A., Lv, J., & Calamante, F. (2022). New insights into anatomical connectivity along the anterior–posterior axis of the human hippocampus using in vivo quantitative fibre tracking. *eLife*, *11*, e76143. https://doi.org/10.7554/eLife.76143

Dalton, M. A., & Maguire, E. A. (2017). The pre/parasubiculum: A hippocampal hub for scene-based cognition? *Current Opinion in Behavioral Sciences*, *17*, 34–40. https://doi.org/10.1016/j.cobeha.2017.06.001

Dalton, M. A., Zeidman, P., McCormick, C., & Maguire, E. A. (2018). Differentiable Processing of Objects, Associations, and Scenes within the Hippocampus. *The Journal of Neuroscience*, *38*(38), 8146–8159. https://doi.org/10.1523/JNEUROSCI.0263-18.2018

Epstein, R. A., Patai, E. Z., Julian, J. B., & Spiers, H. J. (2017). The cognitive map in humans: Spatial navigation and beyond. *Nature Neuroscience*, *20*(11), 1504–1513. https://doi.org/10.1038/nn.4656

Fragueiro, A., Committeri, G., & Cury, C. (2023). Incomplete Hippocampal Inversion and Hippocampal Subfield Volumes: Implementation and Inter-Reliability of Automatic Segmentation. *2023 IEEE 20th International Symposium on Biomedical Imaging (ISBI)*, 1–5. https://doi.org/10.1109/ISBI53787.2023.10230555

Fu, T.-Y., Ho, C.-R., Lin, C.-H., Lu, Y.-T., Lin, W.-C., & Tsai, M.-H. (2021). Hippocampal Malrotation: A Genetic Developmental Anomaly Related to Epilepsy? *Brain Sciences*, *11*(4). https://doi.org/10.3390/brainsci11040463

Grande, X., Sauvage, M. M., Becke, A., Düzel, E., & Berron, D. (2022). Transversal functional connectivity and scene-specific processing in the human entorhinal-hippocampal circuitry. *eLife*, *11*. https://doi.org/10.7554/eLife.76479

Hartley, T., Maguire, E. A., Spiers, H. J., & Burgess, N. (2003). The well-worn route and the path less traveled: Distinct neural bases of route following and wayfinding in humans. *Neuron*, *37*(5), 877–888. https://doi.org/10.1016/s0896-6273(03)00095-3

Hodgetts, C. J., Voets, N. L., Thomas, A. G., Clare, S., Lawrence, A. D., & Graham, K. S. (2017). Ultra-High-Field fMRI Reveals a Role for the Subiculum in Scene Perceptual Discrimination. *The Journal of Neuroscience*, *37*(12), 3150–3159. https://doi.org/10.1523/JNEUROSCI.3225-16.2017

Humphrey, T. (1967). The development of the human hippocampal fissure. *Journal of Anatomy*, *101*(Pt 4), 655–676.

Iaria, G., Arnold, A. E. G. F., Burles, F., Liu, I., Slone, E., Barclay, S., Bech-Hansen, T. N., & Levy, R. M. (2014). Developmental topographical disorientation and decreased hippocampal functional connectivity: Dtd and Hippocampal Functional Connectivity. *Hippocampus*, *24*(11), 1364–1374. https://doi.org/10.1002/hipo.22317

Iaria, G., & Barton, J. J. S. (2010). Developmental topographical disorientation: A newly discovered cognitive disorder. *Experimental Brain Research*, *206*(2), 189–196. https://doi.org/10.1007/s00221-010-2256-9

Iaria, G., Bogod, N., Fox, C. J., & Barton, J. J. S. (2009). Developmental topographical disorientation: Case one. *Neuropsychologia*, *47*(1), 30–40. https://doi.org/10.1016/j.neuropsychologia.2008.08.021

Iaria, G., & Burles, F. (2016). Developmental Topographical Disorientation. *Trends in Cognitive Sciences*, *20*(10), 720–722. https://doi.org/10.1016/j.tics.2016.07.004

Iaria, G., Chen, J.-K., Guariglia, C., Ptito, A., & Petrides, M. (2007). Retrosplenial and hippocampal brain regions in human navigation: Complementary functional contributions to the formation and use of cognitive maps: Retrosplenial cortex and hippocampus in navigation. *European Journal of Neuroscience*, *25*(3), 890–899. https://doi.org/10.1111/j.1460-9568.2007.05371.x

Iglesias, J. E., Augustinack, J. C., Nguyen, K., Player, C. M., Player, A., Wright, M., Roy, N., Frosch, M. P., McKee, A. C., Wald, L. L., Fischl, B., & Van Leemput, K. (2015). A computational atlas of the hippocampal formation using ex vivo , ultra-high resolution MRI: Application to adaptive segmentation of in vivo MRI. *NeuroImage*, *115*, 117–137. https://doi.org/10.1016/j.neuroimage.2015.04.042

Iglesias, J. E., Van Leemput, K., Augustinack, J., Insausti, R., Fischl, B., & Reuter, M. (2016). Bayesian longitudinal segmentation of hippocampal substructures in brain MRI using subject-specific atlases. *NeuroImage*, *141*, 542–555. https://doi.org/10.1016/j.neuroimage.2016.07.020

Kier, E. L., Kim, J. H., Fulbright, R. K., & Bronen, R. A. (1997). *Embryology of the Human Fetal Hippocampus: MR Imaging, Anatomy, and Histology*. 8.

Kim, H., Chupin, M., Colliot, O., Bernhardt, B. C., Bernasconi, N., & Bernasconi, A. (2012). Automatic hippocampal segmentation in temporal lobe epilepsy: Impact of developmental abnormalities. *NeuroImage*, *59*(4), 3178–3186. https://doi.org/10.1016/j.neuroimage.2011.11.040

Kim, J. G., Aminoff, E. M., Kastner, S., & Behrmann, M. (2015). A Neural Basis for Developmental Topographic Disorientation. *Journal of Neuroscience*, *35*(37), 12954–12969. https://doi.org/10.1523/JNEUROSCI.0640-15.2015

Kravitz, D. J., Saleem, K. S., Baker, C. I., & Mishkin, M. (2011). A new neural framework for visuospatial processing. *Nature Reviews Neuroscience*, *12*(4), Article 4. https://doi.org/10.1038/nrn3008

Maller, J. J., Réglade-Meslin, C., Chan, P., Daskalakis, Z. J., Thomson, R. H. S., Anstey, K. J., Budge, M., Sachdev, P., & Fitzgerald, P. B. (2011). Hippocampal sulcal cavities: Prevalence, risk factors and relationship to memory impairment. *Brain Research*, *1368*, 222–230. https://doi.org/10.1016/j.brainres.2010.10.089

Morris, R. G. M., Schenk, F., Tweedie, F., & Jarrard, L. E. (1990). Ibotenate Lesions of Hippocampus and/or Subiculum: Dissociating Components of Allocentric Spatial Learning. *The European Journal of Neuroscience*, *2*(12), 1016–1028. https://doi.org/10.1111/j.1460-9568.1990.tb00014.x

Naber, P. A., Witter, M. P., & Lopes Silva, F. H. (2000). Networks of the hippocampal memory system of the rat. The pivotal role of the subiculum. *Annals of the New York Academy of Sciences*, *911*, 392–403. https://doi.org/10.1111/j.1749-6632.2000.tb06739.x

O'Keefe, J., & Nadel, L. (1978). The Hippocampus as a Cognitive Map. In *Oxford University Press: Oxford, UK. (1978)*. Oxford University Press. http://www.cognitivemap.net/

Stiers, P., Fonteyne, A., Wouters, H., D'Agostino, E., Sunaert, S., & Lagae, L. (2010). Hippocampal malrotation in pediatric patients with epilepsy associated with complex prefrontal dysfunction. *Epilepsia*, *51*(4), 546–555. https://doi.org/10.1111/j.1528-1167.2009.02419.x

Sun, Y., Jin, S., Lin, X., Chen, L., Qiao, X., Jiang, L., Zhou, P., Johnston, K. G., Golshani, P., Nie, Q., Holmes, T. C., Nitz, D. A., & Xu, X. (2019). CA1-projecting subiculum neurons facilitate object-place learning. *Nature Neuroscience*, *22*(11), 1857–1870. https://doi.org/10.1038/s41593-019-0496-y

Swanson, L. W., & Cowan, W. M. (1977). An autoradiographic study of the organization of the efferet connections of the hippocampal formation in the rat. *Journal of Comparative Neurology*, *172*(1), 49–84. https://doi.org/10.1002/cne.901720104

Uttner, I., Weber, S., Freund, W., Bengel, D., Schmitz, B., Ludolph, A. C., & Huber, R. (2011). Hippocampal cavities are not associated with cognitive impairment in transient global amnesia. *European Journal of Neurology*, *18*(6), 882–887. https://doi.org/10.1111/j.1468-1331.2010.03310.x

Van Essen, D. C., Smith, S. M., Barch, D. M., Behrens, T. E. J., Yacoub, E., & Ugurbil, K. (2013). The WU-Minn Human Connectome Project: An overview. *NeuroImage*, *80*, 62–79. https://doi.org/10.1016/j.neuroimage.2013.05.041

Vichot, F., Cochet, H., Bleuzé, B., Toussaint, N., Jaïs, P., & Sermesant, M. (2012). Cardiac Interventional Guidance using Multimodal Data Processing and Visualisation: medInria as an Interoperability Platform. *The MIDAS Journal*. https://doi.org/10.54294/n5h1u5

Weniger, G., & Irle, E. (2006). Posterior parahippocampal gyrus lesions in the human impair egocentric learning in a virtual environment. *The European Journal of Neuroscience*, *24*(8), 2406–2414. https://doi.org/10.1111/j.1460-9568.2006.05108.x

Weniger, G., Siemerkus, J., Schmidt-Samoa, C., Mehlitz, M., Baudewig, J., Dechent, P., & Irle, E. (2010). The human parahippocampal cortex subserves egocentric spatial learning during navigation in a virtual maze. *Neurobiology of Learning and Memory*, *93*(1), 46–55. https://doi.org/10.1016/j.nlm.2009.08.003

Wickham, H. (2009). *ggplot2: Elegant Graphics for Data Analysis*. Springer. https://doi.org/10.1007/978-0-387-98141-3

Witter, M. P., Naber, P. A., van Haeften, T., Machielsen, W. C. M., Rombouts, S. A. R. B., Barkhof, F., Scheltens, P., & Lopes da Silva, F. H. (2000). Cortico-hippocampal communication by way of parallel parahippocampal-subicular pathways. *Hippocampus*, *10*(4), 398–410. https://doi.org/10.1002/1098-1063(2000)10:4<398::AID-HIPO6>3.0.CO;2-K

Witter, M. P., Wouterlood, F. G., Naber, P. A., & Van Haeften, T. (2006). Anatomical Organization of the Parahippocampal-Hippocampal Network. *Annals of the New York Academy of Sciences*, *911*(1), 1–24. https://doi.org/10.1111/j.1749-6632.2000.tb06716.x

Yoneoka, Y., Kwee, I. L., Fujii, Y., & Nakada, T. (2002). Criteria for normalcy of cavities observed within the adult hippocampus: High-resolution magnetic resonance imaging study on a 3.0-T system. *Journal of Neuroimaging: Official Journal of the American Society of Neuroimaging*, *12*(3), 231–235.

Table 1. Descriptive information of all the groups.

Group	N	Age (years)	Behavioural assessment	MRI scanner
DTD	20 females	(range=25 to 64) mean=47.15±11.86	No psychiatric or neurological disorders, assessed as DTD.	3T GE Discovery 750
HC1	220 females	N=213 (range=26-30) N=7 (range > 36)	Human Connectome Dataset WU-Minn. No major neurological diseases, psychiatric or medical disorders.	Siemens 3T "Connectome Skyra"
HC2	18 females	(range=25 to 64) mean=39.61±13.74	No psychiatric or neurological disorders, assessed as no-DTD.	3T GE Discovery 750

Table 2. Mean kappa scores and confidence intervals across all criteria for intra- and inter-rater agreement evaluation.

	AF - AF	***AF - CC***	***AF - FS***
Mean kappa score across all criteria	0.90	0.80	0.74
Confidence interval at 95%	0.85 – 0.96	0.75 – 0.84	0.71 – 0.78

Table 3. Correlation scores between age and volumes, and between age and IHI global scores.

Age		Volumes	Spearman's rho	Uncorrected p-value
	Left	*CA1*	0.028	0.870
		CA2/3/4/DG	0.121	0.468
		Subiculum	0.066	0.695
		Fissure	0.060	0.721
		Tail	0.178	0.286
		Hippocampal body	0.284	0.084
		Hippocampal head	-0.152	0.361
		Whole hippocampus	0.095	0.569
	Right	*CA1*	-0.073	0.664
		CA2/3/4/DG	-0.136	0.417
		Subiculum	0.185	0.265
		Fissure	0.203	0.221
		Tail	0.156	0.350
		Hippocampal body	0.223	0.179
		Hippocampal head	-0.165	0.323
		Whole hippocampus	0.055	0.742
		Incomplete Hippocampal Inversion (IHI)	**Spearman's rho**	**Uncorrected p-value**
	Left	*Global IHI score*	-0.134	0.423
	Right	*Global IHI score*	0.059	0.725

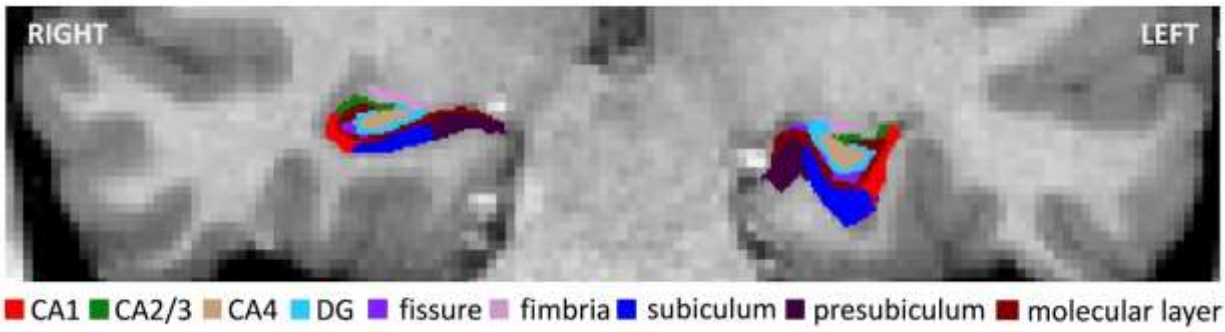

Figure 1. Example of subfields segmentation at the level of the hippocampal body. In this brain, the left hippocampus was rated as IHI.

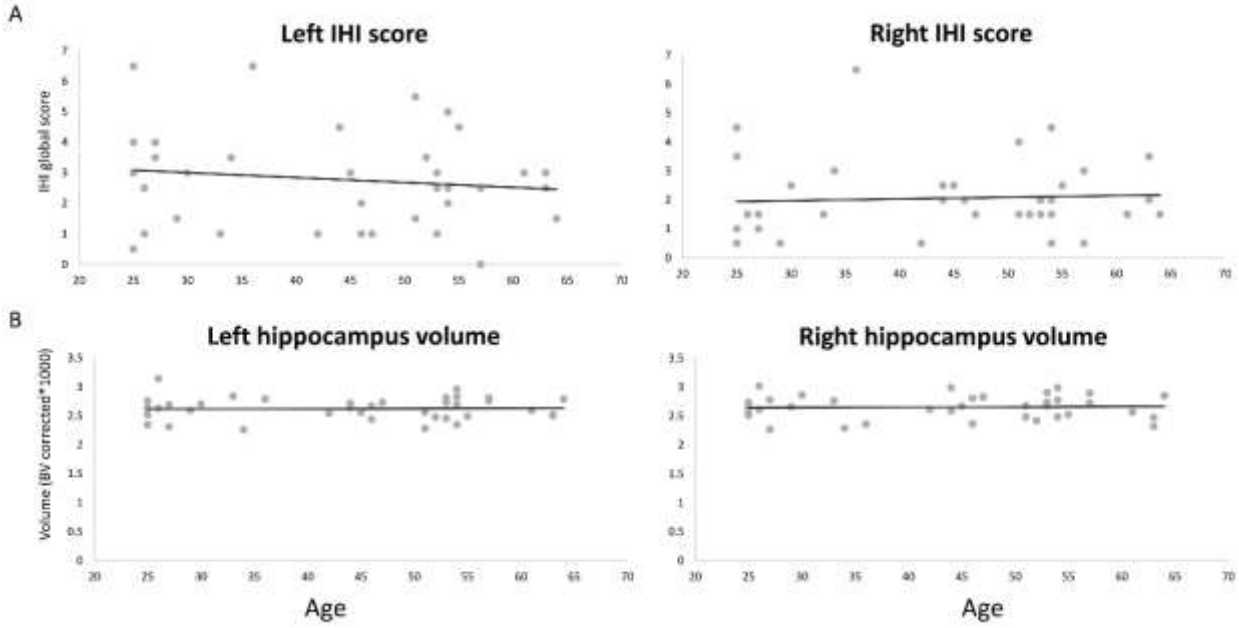

Figure 2. Correlation plots between age and: A) left and right global IHI scores (Left: rho=-13.4, p=0.423; Right: rho=0.059, p=0.725); B) left and right whole hippocampal volumes (Left: rho=0.095, p=0.569; Right: rho=0.055, p=0.742), including participants from the HC2 and DTD groups.

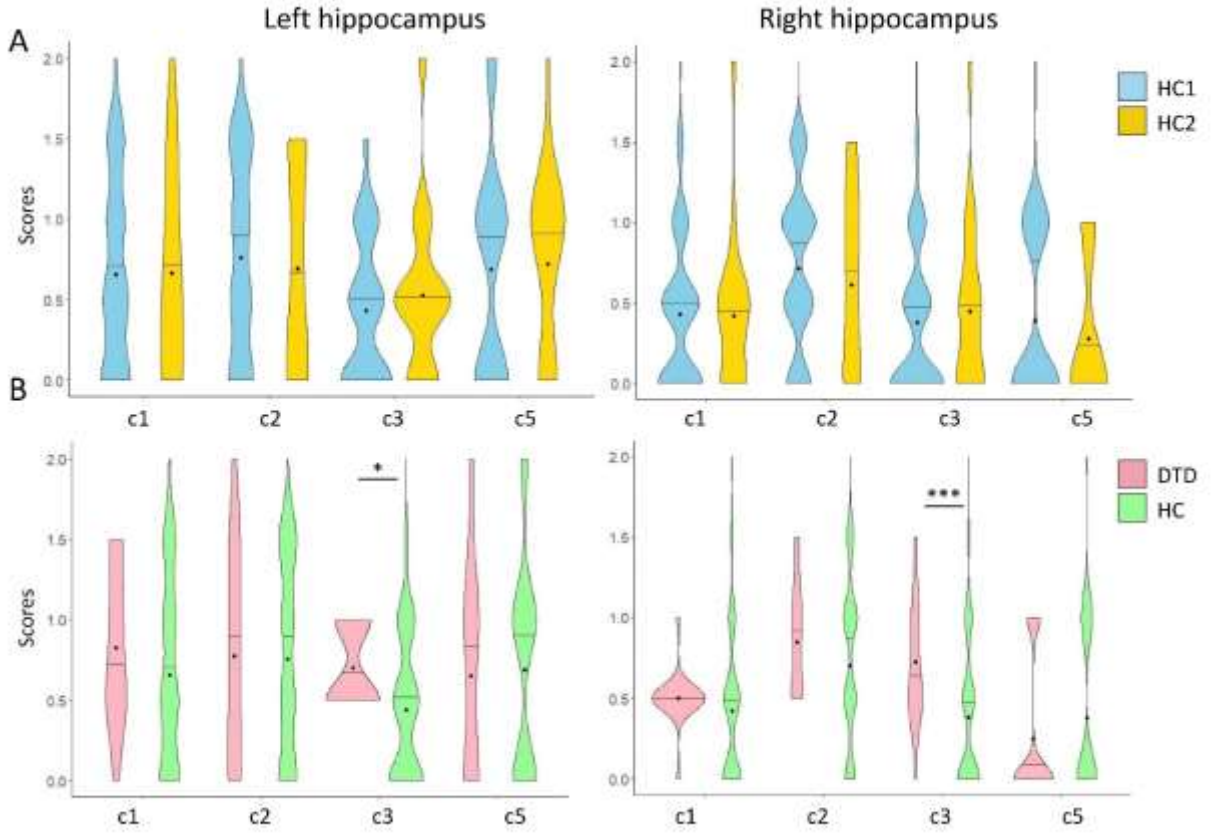

Figure 3. Violin plots depicting the differences in score for each IHI independent criterion between: A) HC1 and HC2, and B) HC and DTD groups. The black line represents the quantile 0.5, while the black point corresponds to the mean. *p<0.05, **p<0.01, Bonferroni corrected.

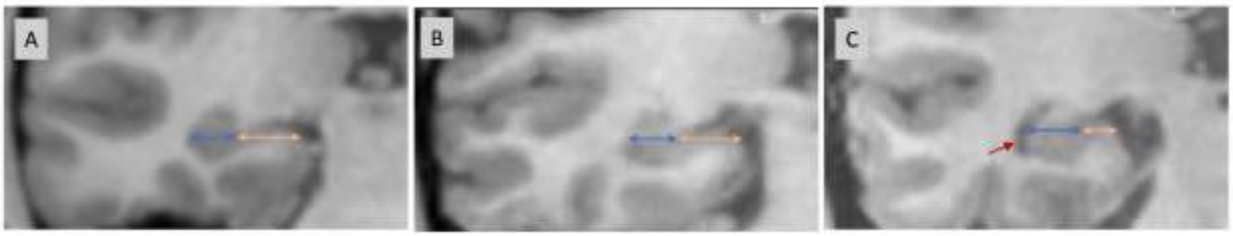

Figure 4. Example of three right hippocampi for criteria 3, all of them after linear MNI transformation. A) Image from the HC1 database with a score of 0 for criteria 3 on the right hemisphere; B) image from the HC2 database with a score of 0 for criteria 3; C) image from the DTD database with a score of 1.5 for criteria 3, as the hippocampus is more medially positioned and the temporal horn of the lateral ventricle is filled with cerebrospinal fluid. Orange arrows indicate the part of the subiculum that is not covered by the dentate gyrus. Blue arrows indicate the part of CA/subiculum that is covered by the dentate gyrus. The red arrow indicates presence of cerebrospinal fluid in the temporal horn.

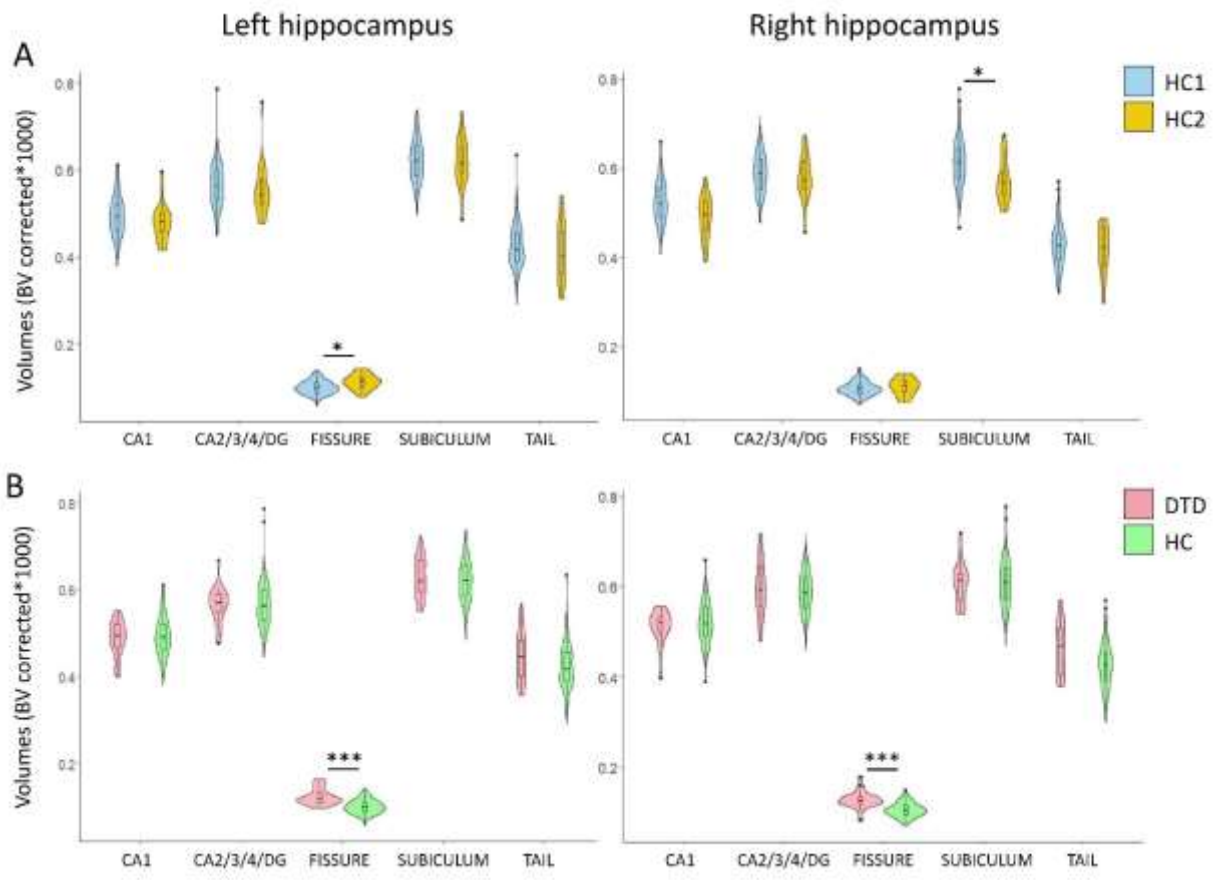

Figure 5. Violin plots overlapped with the corresponding boxplots comparing hippocampal subfield volumes between: A) HC1 and HC2, and B) HC and DTD groups. BV=brain volume. * $p \leq 0.05$, *** $p < 0.001$, Bonferroni corrected.

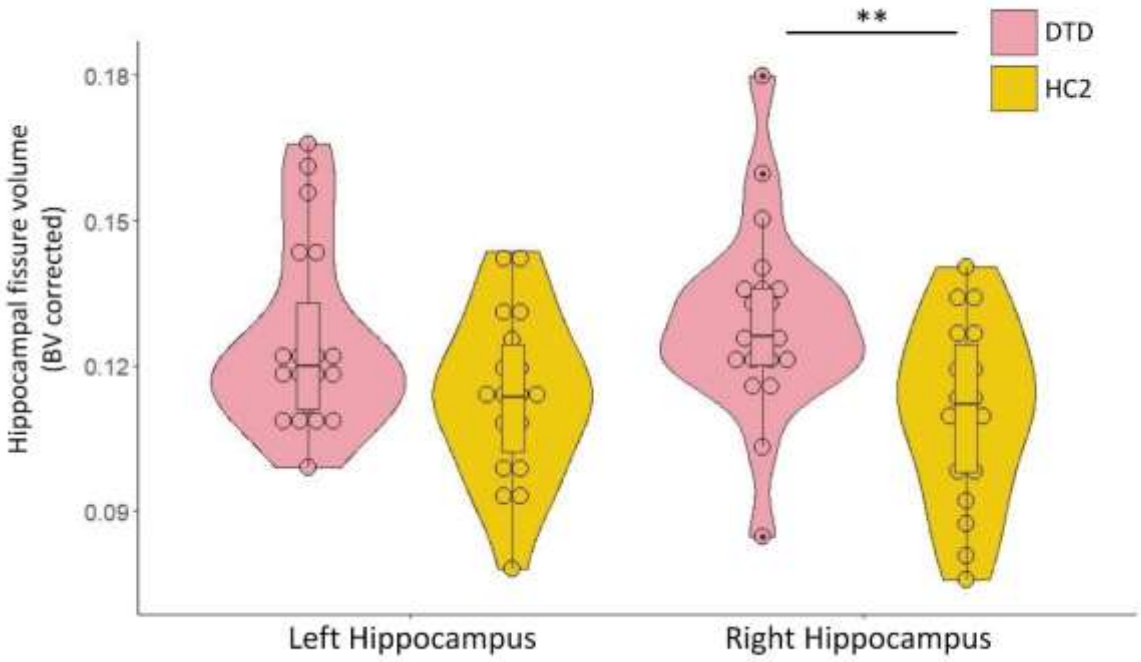

Figure 6. Violin plots overlapped with the corresponding boxplots and dot plots comparing hippocampal fissure volumes between HC2 and DTD groups. **p ≤0.01, Bonferroni corrected.